Dalton Transactions

ROYAL SOCIETY OF CHEMISTRY

PAPER

View Article Online
View Journal

Cite this: DOI: 10.1039/d5dt02949j

Synthesis of heteroleptic calcium amide complexes *via* manipulation of the Schlenk equilibrium

Matthew de Vere-Tucker, [a,b] Alexandra M. Z. Slawin, [b] David B. Cordes [b] and Andreas Stasch *[b]

Heteroleptic calcium β-diketiminate (BDI) complexes have been recognised as potent (pre)catalysts for a variety of transformations and have demonstrated valuable stoichiometric reactivity. Bulky ligands such as BDIs have been utilised to prevent unwanted dismutation and decomposition reactions of active heteroleptic species to their homoleptic congeners. Homoleptic bis-ligated alkaline earth metal (Ae) species of the type "L_2Ae" have hitherto been often considered kinetic sinks and less valuable by-products. This work shows that through the use of the sterically demanding proligand $HC(iPrCNDip)_2H$, Dip = 2,6-$iPr_2C_6H_3$ (^{iPrDip}BDIH), the homoleptic calcium complex [(^{iPrDip}BDI)$_2$Ca] can be destabilised to the degree that when treated with calcium bis(hexamethyldisilazide) ($Ca(HMDS)_2$), a thermal dismutation of the ligands takes place to afford the heteroleptic complex [(^{iPrDip}BDI)Ca(HMDS)]. DFT calculations support that this reaction is enthalpically unfavourable, an effect that is reduced by the destabilising influence of the bulk in [(^{iPrDip}BDI)$_2$Ca], but entropically made possible. This synthesis has been extended to a convenient one-pot regime from [(^{iPrDip}BDI)K], CaI_2 and $Ca(HMDS)_2$, and the resultant calcium amide complex has been utilised as a precursor to prepare a thermally stable, donor-solvent-free molecular calcium hydride complex [{(^{iPrDip}BDI)CaH}$_2$].

Received 9th December 2025,
Accepted 23rd December 2025

DOI: 10.1039/d5dt02949j

rsc.li/dalton

1. Introduction

Heteroleptic complexes of alkaline earth (Ae) metals are strongly prone to Schlenk-type redistribution reactions.[1,2] These were first described by Schlenk and Schlenk Jr in 1929 as it was observed that an ethereal solution of a Grignard reagent contained not only the RMgX species (where R is an alkyl or aryl substituent and X is a halide), but also the R_2Mg and MgX_2 species.[3] The Schlenk equilibrium (Fig. 1) manifests itself due to the predominant ionic nature of the bonds between the metal ion and the coordinated ligands.[4] These are generally easy to distort, which allows the relatively facile formation and breaking of coordination bonds. As the metal ion size increases down a group, the propensity towards Schlenk-type redistribution increases, leading to faster ligand exchange rates and often greater instability of heteroleptic complexes. Furthermore, purely inorganic AeX_2-type species have high lattice energies, which can further drive Schlenk-type redistribution to one side. This is due to the precipitation of the AeX_2 species from solution and thus the equilibrium is driven towards the redistributed species. Related to the use of Ae metal complexes in catalysis, active heteroleptic complexes can be generated *in situ* from homoleptic precatalyst complexes and are then subject to these equilibria.[1,2]

In addition, when LAeX species (where L is a sterically demanding anionic spectator ligand) dismutate, the resultant L_2Ae species are generally considered to be kinetically inert. As such, both the often valuable ligand entity, L, and the reactive fragment, X, *e.g.* a metal hydride moiety, can be lost for the desired reactivity, for example, as part of catalytic processes. This redistribution can be prevented by kinetically suppressing exchange processes, or by manipulating the position of the equilibrium through donor–solvent effects.[5,6] β-Diketiminate (BDI) ligands are ubiquitous *N*,*N*′-chelating ligands in main group chemistry and are particularly widely used in Ae metal chemistry for their strong stabilising characteristic.[7–13] BDI ligand-stabilised calcium complexes have applications in catalysis,[14–20] and recently have been used as precursors for low-valent synthons.[21–25] Calcium hydride complexes are a par-

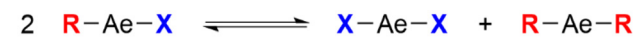

Fig. 1 Simplified Schlenk-type equilibrium.

[a]Department of Chemistry, King's College London, 7 Trinity Street, London, SE1 1DB, UK
[b]EaStCHEM School of Chemistry, University of St Andrews, North Haugh, KY16 9ST St Andrews, UK. E-mail: as411@st-andrews.ac.uk

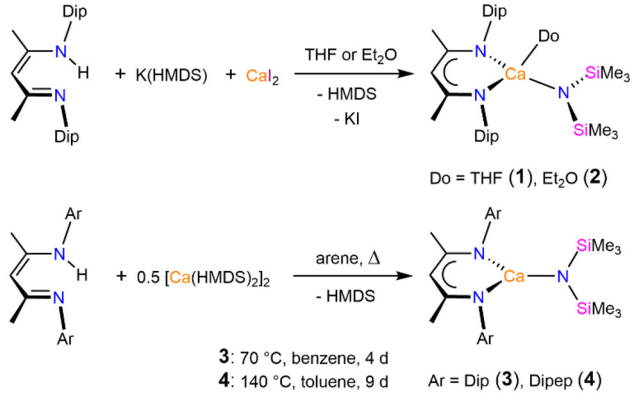

Scheme 1 Reported syntheses of (BDI)Ca(HMDS) complexes; HMDS = $N(SiMe_3)_2$.

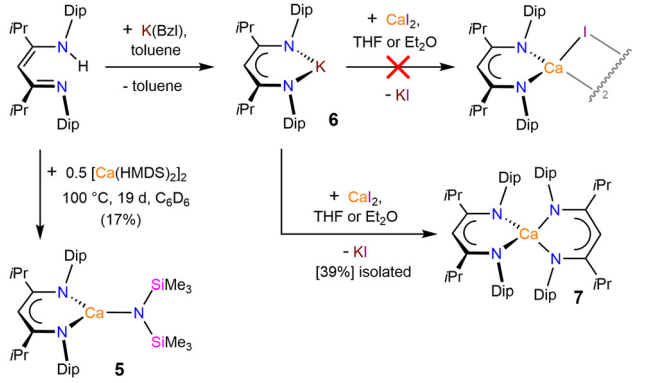

Scheme 2 Synthesis of homoleptic complex [(^{iPrDip}BDI)$_2$Ca] (**7**).

ticularly rich field of exploration, with molecular calcium hydride species demonstrating rich and potent stoichiometric and catalytic reactivity.[26–34]

A key precursor to the synthesis of calcium hydride complexes is typically a calcium HMDS species (HMDS = hexamethyldisilazide, $N(SiMe_3)_2$). For BDI ligand-stabilised calcium HMDS complexes, there are two synthetic routes available, see Scheme 1. One approach is the treatment of the proligand with KHMDS to effect the *in situ* deprotonation and subsequent salt metathesis with CaI_2 in an ethereal solvent[35,36] to afford donor solvent adducts such as [(^{MeDip}BDI)Ca(HMDS)(THF)] **1** and [(^{MeDip}BDI)Ca(HMDS)(OEt_2)] **2** (^{MeDip}BDI = HC(MeCNDip)$_2$; Dip = 2,6-diisopropylphenyl). Another route utilises direct deprotonation of a suitable BDIH proligand with $Ca(HMDS)_2$ to afford complexes such as [(^{MeDip}BDI)Ca(HMDS)] **3** and [(^{MeDipep}BDI)Ca(HMDS)] **4** (^{MeDipep}BDI = HC(MeCNDipep)$_2$; Dipep = 2,6-bis(3-pentyl)phenyl).[37] The latter route, while slower, has the advantage of avoiding coordinating solvents and halide salts.

We have recently developed a facile route to the synthesis of the isopropyl-substituted proligand ^{iPrDip}BDIH[38,39] (= HC(iPrCNDip)$_2$H) which we have employed for the stabilisation of a range of highly reactive magnesium species that highlighted the impact and importance of backbone substituent modifications.[39,40] Here we demonstrate these substituent effects on the synthetic accessibility and stability of heteroleptic calcium amide and hydride complexes.

2. Results and discussion

It was presumed that the treatment of ^{iPrDip}BDIH with $Ca(HMDS)_2$ would yield the desired BDI calcium amide precursor complex [(^{iPrDip}BDI)Ca(HMDS)] **5** *via* an elimination reaction as shown in Scheme 1. However, no significant reaction was observed *via* ^{1}H NMR spectroscopy even when a solution of ^{iPrDip}BDIH and $Ca(HMDS)_2$ was heated in benzene-d_6 to 100 °C for over one week. This resistance to deprotonation was surprising, as ^{MeDip}BDIH is readily deprotonated through its treatment with $Ca(HMDS)_2$.†[37] After nineteen days at 100 °C, resonances presumably corresponding to the formation of complex **5** were observed (*vide infra*); however, only with a conversion of *ca.* 17%, and thus an alternative synthetic route was targeted. It should be noted that this extremely slow reaction is proposed to be likely a result of kinetic factors, as previously shown by other successful attempts to deprotonate ^{iPrDip}BDIH with alkali metal amide bases.[38] It was postulated that the deprotonation was the rate-limiting step and as such a route where ^{iPrDip}BDIH is deprotonated with a more potent base was necessary. Thus, ^{iPrDip}BDIH was treated with a slight excess of benzyl potassium K(Bzl), in deuterated benzene, which, after one hour at room temperature, afforded a red-orange solution (Scheme 2). ^{1}H NMR spectroscopic analysis indicated the formation of the potassium complex [(^{iPrDip}BDI)K] **6**, per the disappearance of the singlet at δ = 12.30 ppm corresponding to the imino proton, the appearance of a resonance for the by-product, toluene, and the characteristic backbone methine resonance at 4.16 ppm.[38]

With the intention of obtaining the heteroleptic calcium iodide species [(^{iPrDip}BDICaI)$_2$], complex **6** was treated with CaI_2 under a variety of conditions, for example heating in an arene solvent, stirring in Et_2O at room temperature, 0 °C and −78 °C or stirring the mixture in THF at room temperature and −78 °C, *etc.*, but a heteroleptic complex of this type was never obtained in any observable quantities. Instead, the only main products obtained were either the proligand ^{iPrDip}BDIH or the homoleptic complex [(^{iPrDip}BDI)$_2$Ca] **7**, see Scheme 2. This salt-metathesis route has previously been used with some success for the synthesis of heteroleptic BDI calcium iodide species with methyl backboned BDI ligands[21,41] and it is notable that the homoleptic complex [(^{MeDip}BDI)$_2$Ca] has previously been reported as a by-product for this process.[41]

The ^{1}H NMR spectrum of [(^{iPrDip}BDI)$_2$Ca] **7** is worthy of comment and is consistent with NMR spectra of other bulky

† The reaction is reported to require 4 days for full conversion when heating to 70 °C in benzene; in our hands, we found that effectively quantitative conversion to [(^{MeDip}BDI)Ca(HMDS)] **3** was achieved after heating the mixture for 16 hours at 80 °C in toluene.

homoleptic alkaline earth metal BDI species.[42] The high degree of steric crowding of complex 7 is evidenced by the splitting of the isopropyl methyl and methine resonances resulting into six septets and twelve doublets, corresponding to the methine and methyl groups, respectively, rather than the usual three doublets and two septets as would be expected for ^{iPrDip}BDI-stabilised complexes, where the solution-averaged structure shows one ^{iPrDip}BDIM environment with equivalence above and below the NCCCN plane and across the left- and right-hand sides of the ligand moiety. This highly asymmetric ligand environment in the solution state is due to the crowded and interlocked nature of the complex. There is a substantial twist in the NCCCN plane observed in the solid-state structure (*vide infra*) which appears to be retained in solution and thus results in the unusual separation of the backbone isopropyl resonances. The two ligands themselves are equivalent according to NMR spectroscopy, as evidenced by the single backbone methine resonance. Storage of a saturated diethyl ether solution of complex 7 for several days at −40 °C afforded single crystals suitable for X-ray crystallography, see Fig. 2 and 3. Complex [(^{iPrDip}BDI)$_2$Ca]·OEt$_2$, 7·OEt$_2$, crystallised in the triclinic space group $P\bar{1}$ with a full molecule and one equivalent of diethyl ether in the asymmetric unit. The calcium atom is coordinated in a distorted tetrahedral fashion by the two *N,N*-chelating BDI ligands, which are approximately orthogonal to one another with respect to their NCaN least-square planes (82.2(9)°). The significant steric strain of this complex is exemplified by the displacement of the Ca from the two NCCCN least square planes, 1.497(3) and 1.522(3) Å, respectively. These values are greater than those of [(^{MeDip}BDI)$_2$Ca][35,42,43] and notably, given the smaller ionic radius of calcium compared to strontium and barium,[44] larger than that of the strontium and barium complexes [(^{MeDip}BDI)$_2$Ae] (Ae = Sr, Ba) (Ca = 1.291 Å, Sr = 1.381 Å and Ba = 1.498, 0.946 Å). The Ca–N bond distances range from 2.383(2) to 2.418(2) Å, which are slightly larger than those of [(^{MeDip}BDI)$_2$Ca] (2.374 and 2.384 Å). The coordination environment around Ca, as judged by the τ_4 values, is slightly less tetrahedral for 7 (0.74) compared with [(^{MeDip}BDI)$_2$Ca] (0.78). The steric strain and interlocking of the substituents in complex 7 can be visualised in the space-filling model, Fig. 3, which also points to the substantial stabilisation from dispersion between substituents. The twisting and distortion of the iPrCC(H)CiPr backbone units, *e.g.* the central turquoise unit shown in Fig. 3, are due to the steric congestion, but it is worth pointing out that the BDI backbone methine C(H) unit (centre of Fig. 3) that can act as a coordination site, is visible.

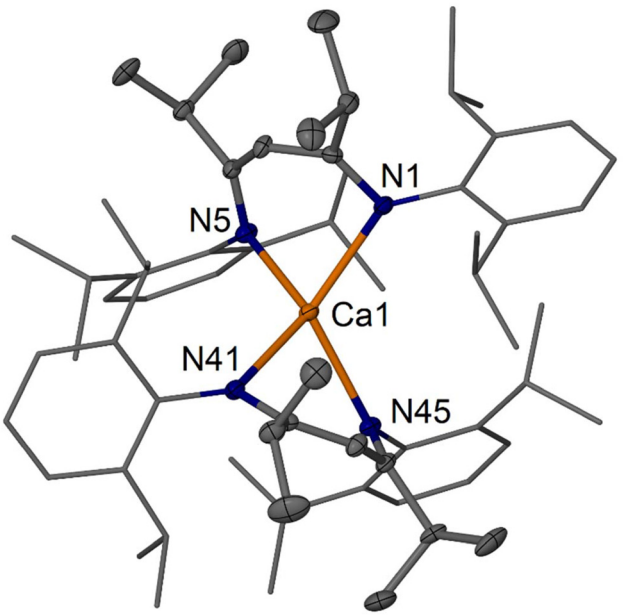

Fig. 2 Molecular structure of [(^{iPrDip}BDI)$_2$Ca]·OEt$_2$, 7·OEt$_2$ (thermal ellipsoids with 30% probability, hydrogen and solvent atoms omitted for clarity). The Dip-substituents are shown as wireframe only. Selected bond lengths (Å) and angles (°): Ca1–N1 2.383(2), Ca1–N5 2.412(2), Ca1–N41 2.389(3), Ca1–N45 2.418(2); N1–Ca1–N5 85.13(8), N41–Ca1–N45 85.13(8), N1–Ca1–N41 132.06(8), N1–Ca1–N45 118.49(8), N41–Ca1–N5 118.20(9), N5–Ca1–N45 122.66(9).

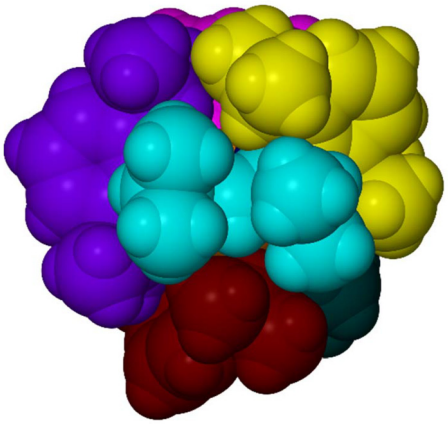

Fig. 3 Space-filling (van der Waals) model of the molecular structure of [(^{iPrDip}BDI)$_2$Ca]·OEt$_2$, 7·OEt$_2$, without the solvent molecule. The iPrCC(H)CiPr backbone units are turquoise (on N41, N45) and dark green (on N1, N5), and the Dip substituents are yellow (on N41), purple (on N45), dark red (on N1) and magenta (on N5); Ca is orange and N atoms are blue but are hardly visible in this view.

The apparent substantial steric strain in complex 7 prompted speculation that the ^{iPrDip}BDI ligands may engage in ligand exchange reactions at high temperatures. As such, a deuterated benzene solution of 7 was treated with one equivalent of Ca(HMDS)$_2$ and the mixture was heated to 100 °C for 12 hours. ^{1}H NMR spectra of the mixture after this period show the resolution of the six septets and twelve doublets down to resonances for a new compound with two septets and three doublets, indicating the full consumption of complex 7 and suggesting the formation of a sterically less congested species, see Scheme 3. Furthermore, loss of the resonance at δ = 0.32 ppm corresponding to the Ca(HMDS)$_2$ hydrogens and the appearance of a resonance at δ = 0.12 ppm (consistent with that observed for [(^{MeDip}BDI)Ca(HMDS)][36]), indicate the for-

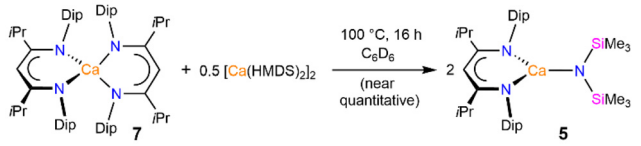

Scheme 3 Synthesis of [(^{iPrDip}BDI)Ca(HMDS)] **5**.

mation of [(^{iPrDip}BDI)Ca(HMDS)] **5**. Storage of a saturated *n*-hexane solution of **5** at −40 °C afforded large crystals of the donor solvent-free complex [(^{iPrDip}BDI)Ca(HMDS)] **5**, see Fig. 4, whereas storage of a concentrated diethyl ether solution of **5** afforded large crystals of the diethyl ether adduct [(^{iPrDip}BDI)Ca(HMDS)(OEt_2)] **8**, Fig. 5.

Compounds [(^{iPrDip}BDI)Ca(HMDS)] **5**, [(^{iPrDip}BDI)Ca(OEt_2)(HMDS)]$_2$ **8** and the highly similar solvate [(^{iPrDip}BDI)Ca(OEt_2)(HMDS)]·OEt_2, **8**·OEt_2, see Fig. S15, all crystallised with one main molecule in the asymmetric unit in a monoclinic crystal system. Comparing the molecular structures of complexes **5**, **8** and [(^{iPrDip}BDI)$_2$Ca] **7** with their ^{MeDip}BDI counterparts (**3**, **2** and [(^{MeDip}BDI)$_2$Ca]) revealed highly comparable Ca–N bond lengths, with marginally longer bonds observed for the solvated species, as would be expected. The bulkier backbone units in **5** and **8** appear slightly more twisted compared with their ^{MeDip}BDI-analogues. The N1–Ca1–N5 bond angle in **5** (84.87(4)°) is somewhat wider than that of **8** (82.07(3)°) and **3** (82.11(11)°) and both are slightly narrower than those of **7** (85.13(9) and 85.10(9)°). The sum of the three N–Ca–N bond angles in **5** (360.0(1)°) shows planarity, whereas that of **8** (345.2(1)°) is closer to planar than tetrahedral geometry. The most dramatic difference between **5** and **8** is in the magnitude of the deviation of Ca from the NCCCN least-square plane, which for **5** is 1.5145(16) Å, which is comparable with that of **7** and near double that of **8** (0.7588(14) Å), albeit more consistent with that of **3** (1.333 Å). Also notable is the significant difference in the dihedral angle of the Ca–NSi_2 unit in **8**, which at 28.1(3)° is approaching coplanarity with the *β*-diketiminate moiety due to the Et_2O ligand, whereas for **5** it is nearly orthogonal at 85.38(10)°. Unlike in the packing of [(^{MeDip}BDI)Ca(HMDS)] **3**, only weak intramolecular interactions are observed in **5**, including Ca···H(iPr) (shortest: 2.7550(5) Å) and Ca···H(Me_3SiN) (shortest: 2.8124(6) Å), and Si–N–Ca angles of 111.60(7) and 116.77(7)°. The buried volumes (V_{bur})[45,46] of the ^{iPrDip}BDI ligands were calculated to be 49.4% for **5** and 45.5% for **8** – perhaps counterintuitively, but as the Ca centre deviates from the ligand plane in **5** it is brought closer to the isopropyl groups. The calculated V_{bur} for **5** is notably greater than that of **3** (46.9%).

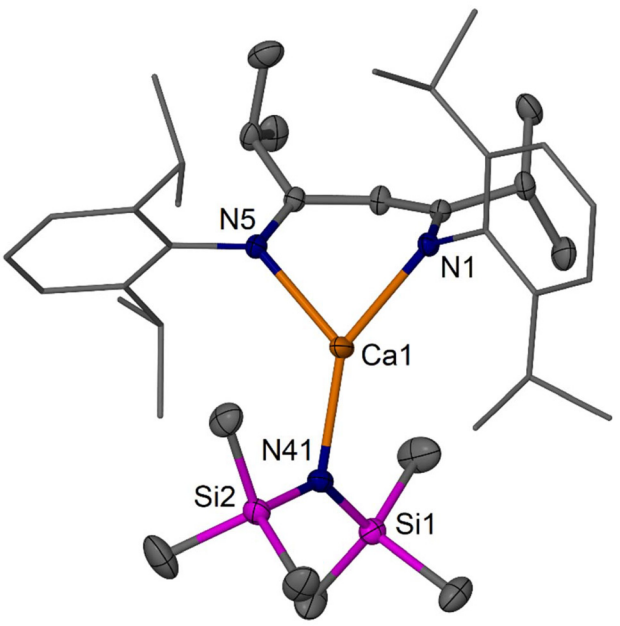

Fig. 4 Molecular structure of compound [(^{iPrDip}BDI)Ca(HMDS)] **5** (thermal ellipsoids with 30% probability, hydrogen and solvent atoms omitted for clarity). The Dip-substituents are shown as wireframe only. Selected bond lengths (Å), and angles (°): Ca1–N1 2.3131(12), Ca1–N5 2.3128(13), Ca1–N41 2.2631(13), Si1–N41 1.6804(14), Si2–N41 1.6796(14); N5–Ca1 N1 84.87(4), N41–Ca1–N1 147.55(5), N41–Ca1–N5 127.55(5), Si1–N41–Ca1 116.77(7), Si2–N41–Ca1 111.60(7), Si2–N41–Si1 131.55(8).

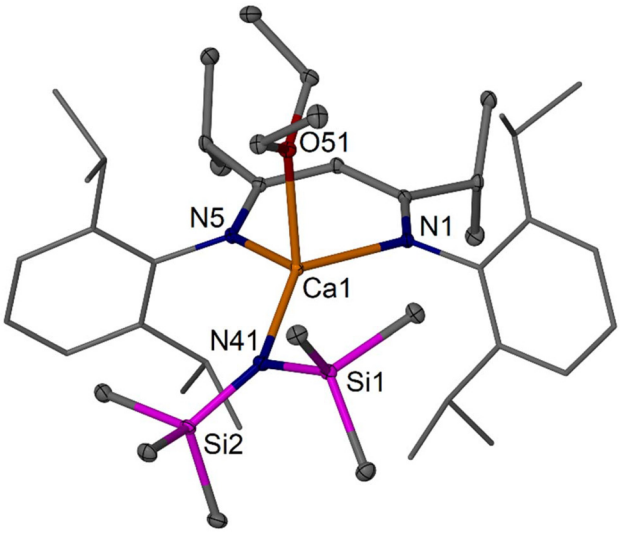

Fig. 5 Molecular structure of [(^{iPrDip}BDI)Ca(HMDS)(OEt_2)] **8** (thermal ellipsoids with 30% probability, hydrogen and solvent atoms omitted for clarity). The Dip-substituents are shown as wireframe only. Selected bond lengths (Å) and angles (°): Ca1–N1 2.4239(9), Ca1–N5 2.3802(9), Ca1–N41 2.3435(9), Ca1–O51 2.3810(8), Si1–N41 1.7096(10), Si2–N41 1.7173(9); N5–Ca1–N1 82.07(3), N41–Ca1–N1 136.49(3), N41–Ca1–N5 126.61(3), N41–Ca1–O51 106.57(3), Si1–N41–Si2 118.67(5), Si2–N41–Ca1 130.02(5), Si1–N41–Ca1 110.81(4).

Due to the low overall isolated yield of complex **7** (39% isolated over three crystalline crops) from the reaction of [(^{iPrDip}BDI)K] **6** with CaI_2 in a 1 : 1 molar ratio at −78 °C in Et_2O, a more convenient synthetic route was sought. A one-pot approach was tested by heating a toluene slurry of [(^{iPrDip}BDI)K] **6**, finely ground CaI_2 and Ca(HMDS)$_2$ to 100 °C for 4 days with rapid stirring, see Scheme 4. This afforded complex **5** as a

pale brown solid in 85% yield after workup. It was hoped that if it was possible to perform this redistribution reaction with sparingly soluble CaI_2 in an arene solvent, then perhaps it could be possible to directly treat the homoleptic complex **7** with commercial $(CaH_2)_\infty$ to afford the heteroleptic calcium hydride complex [{(^{iPrDip}BDI)CaH}$_2$] **9**. As such, a deuterated benzene solution of **7** was treated with 10 equivalents of very finely ground $(CaH_2)_\infty$. No reaction was observed, however, even after heating the mixture to 100 °C for seven days. The effective complete insolubility of CaH_2 is likely a significant factor here, coupled with its high lattice energy (−2401 kJ mol^{-1}) that is substantially greater than that of CaI_2 (−1905 kJ mol^{-1}).[47]

Molecular main group hydrides[34,48,49] are of interest due to their intrinsic high reactivity and their range of applications, from catalysis, to energy storage and materials deposition. Calcium hydride complexes are generally synthesised *via* ligand metathesis of the HMDS moiety with a hydride source such as phenylsilane.[21,26,50,51] As such, a deuterated benzene solution of complex **5** was treated with three equivalents of phenylsilane, see Scheme 5. Analysis *via* ^{1}H NMR spectroscopy after 12 hours showed the complete disappearance of the peaks corresponding to **5**, and the formation of a new set of ^{iPrDip}BDI resonances. Singlets are observed at δ = 0.22 ppm, integrating to 18 protons, and δ = 5.16 ppm, integrating to two protons. These are consistent with the formation of $PhSiH_2N(SiMe_3)_2$. Furthermore, an apparent new BDI backbone methine resonance at the more upfield chemical shift of δ = 4.79 ppm is found, as is a broad singlet at δ = 4.29 ppm, which is consistent with that of a hydride moiety, as observed for previously isolated BDI calcium hydride species.[26,50,51] ^{1}H–^{13}C and ^{1}H–^{1}H 2D NMR experiments confirmed that the singlet at δ = 4.29 ppm shows no cross-peaks with any other resonances, as would be expected for a metal hydride resonance, indicating the synthesis of [{(^{iPrDip}BDI)CaH}$_2$] **9**. To obtain isolated material, an *n*-hexane solution of three equivalents of phenylsilane was added dropwise to a stirred *n*-hexane solution of **5** at −78 °C. This afforded a colourless solid and pale green solution. The colourless solid was found to be deuterated benzene soluble and ^{1}H NMR spectroscopic analysis revealed it to be pure complex **9**, afforded in a 42% yield. The donor adduct [{(^{iPrDip}BDI)CaH(OEt$_2$)}$_2$], *cf.* [{(^{MeDip}BDI)CaH(OEt$_2$)}$_2$],[52] was

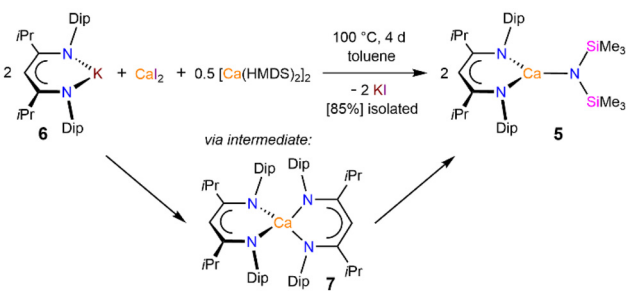

Scheme 4 One-pot synthesis of [(^{iPrDip}BDI)Ca(HMDS)] **5**.

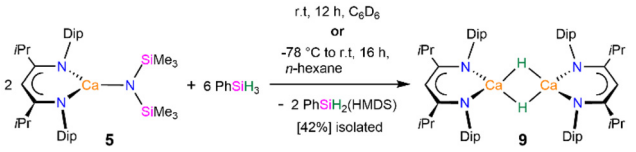

Scheme 5 Synthesis of [{(^{iPrDip}BDI)CaH}$_2$] **9**.

generated *in situ* from [(^{iPrDip}BDI)Ca(HMDS)(OEt$_2$)] **8** in a similar manner but was not isolated.

Crystals of [{(^{iPrDip}BDI)CaH}$_2$] **9** suitable for X-ray diffraction were obtained from the storage of the concentrated supernatant solution. Compound **9** crystallised in the tetragonal space group $I4_1cd$ with half a molecule in the asymmetric unit, see Fig. 6. The crystal structure confirms the proposed dimeric nature of the complex. The mean Ca–N bond length (2.332 Å) of **9** is slightly longer than that of the previously reported [{(^{MeDip}BDI)CaH}$_2$] **10** (2.316 Å). The Ca1···Ca1′ distance in **9** is around 0.1 Å larger, at 3.4566(6) Å *versus* 3.3401(6) Å in **10**. There is negligible deviation (0.182(3) Å) of the Ca from the NCCCN least-square plane (*cf.* 0.437 Å for **10**) and the amide precursor **5** (1.5145(16) Å, *vide supra*). The small hydride ligands in **9** and the relatively planar NCCCNCa-ring also lead to the least twisting of the backbone unit in the characterised series. The dihedral angle about the Ca···Ca axis in **9** (39.69 (7)°) is substantially different to the co-planar arrangement of the two ^{MeDip}BDICa moieties in **10**. The V_{bur} of complex **9** has been determined as 52.4%, which is notably greater than the V_{bur} of **10** (49.5%), and surprisingly, even similar or slightly greater than that of [{(^{Dipep}BDI)CaH}$_2$] **11**[21] (51.8%). This may indicate that the backbone iPr groups provide notable additional steric protection, although care should be taken when closely comparing these numbers as packing effects will

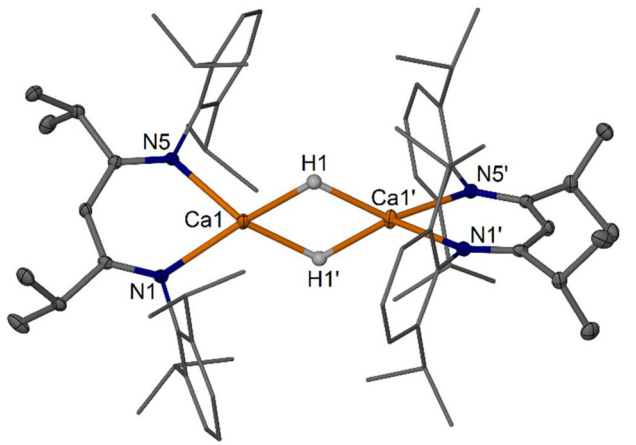

Fig. 6 Molecular structure of [{(^{iPrDip}BDI)CaH}$_2$] **9** (ellipsoids with 30% probability, hydrogen atoms except for H1 and H1′ are omitted). The Dip-substituents are shown as wireframe only. Selected bond lengths (Å) and angles (°): Ca1–N1 2.3324(17), Ca1–N5 2.3316(17), Ca1–H1 2.103(7), Ca1–H1′ 2.22(3), Ca1···Ca1′ 3.4567(9); N5–Ca1–N1 79.75(6), N1–Ca1···Ca1′ 142.79(4), N5–Ca1···Ca1′ 137.23(4).

influence these values. This increased V_{bur} appears not to be simply a function of the isopropyl groups tightening the ligand bite angle with an N–Ca–N angle of 79.75(6)° for **9**, which is essentially identical to that in **11** (79.25(5)°). Comparing the Ca–N–C_{ipso} angles, **9** exhibits a slightly tighter to identical angle (108.87(12)° for Ca–N1–C_{ipso}, 108.29(12)° for Ca–N5–C_{ipso}) compared to those of **11** (109.48(9)° and 110.5(1)°). The steric bulk in **9** is significantly more symmetrically distributed due to the lower steric demand of the hydride ligands compared to the HMDS groups in [(^{iPrDip}BDI)Ca(HMDS)] **5** and [(^{iPrDip}BDI)Ca(HMDS)(OEt$_2$)] **8**, see Fig. S16 and S17.

Preliminary investigations towards the thermal stability of [{(^{iPrDip}BDI)CaH}$_2$] **9** have been carried out, with a deuterated benzene solution of **9** being heated to 100 °C with periodic ^{1}H NMR analysis to determine the rate of decomposition. It was found that **9** has a half-life of approximately 96 hours in benzene at 100 °C (Fig. S13). The stability of [{(^{MeDip}BDI)CaH}$_2$] **10** was probed in addition under the same conditions (Fig. S14), with 50% decomposition largely to [(^{MeDip}BDI)$_2$Ca] observed after *ca.* 30 hours, providing further evidence for the increased complex robustness afforded by the BDI backbone isopropyl groups of **9** compared to the methyl groups of **10**.

For further insights into this apparent reversion of the conventional direction of the Schlenk-type equilibrium towards the formation of the heteroleptic complex [(^{iPrDip}BDI)Ca(HMDS)] **5**, the Gibbs Free Energies for the redistribution reaction of [(^{iPrDip}BDI)$_2$Ca] **7** and Ca(HMDS)$_2$, modelled as the unsolvated dimer [Ca(HMDS)$_2$]$_2$, were investigated by DFT calculations at the B3LYP$_{PCM(benzene)}$/6-311G**//B3LYP/6-31G** level of theory, and compared to the same reaction for the ^{MeDip}BDI ligand, see Fig. 7.

For both cases, the reaction requires a significant investment in reaction enthalpy but becomes viable for entropic reasons, especially at higher temperatures. It was found that in the case of [(^{MeDip}BDI)$_2$Ca] plus Ca(HMDS)$_2$, the formation of the heteroleptic complex [(^{MeDip}BDI)Ca(HMDS)] is approximately energy neutral across the studied temperature range, whereas the formation of [(^{iPrDip}BDI)Ca(HMDS)] **5** from ligand redistribution is exergonic (−25.1 kcal mol^{-1} for the shown reaction, or −6.3 kcal mol^{-1} as referenced to the formation of one mole of **5**) at the reaction temperature of 100 °C for the ligand with the bulkier backbone. The high reaction temperature is likely also required for kinetic reasons. The DFT calculations, in combination with the analysis of the molecular structures, suggest that the backbone modification in the ^{iPrDip}BDI derivatives contribute to the exergonicity of the reaction, for example by the steric crowding and large strain in [(^{iPrDip}BDI)$_2$Ca] **7**, which is expected to lower the ΔH for the reaction by destabilising the homoleptic species. The strain may further contribute to possible differences in kinetic hurdles between both systems, which were not computationally studied, such as more facile decoordination of one N(Dip) arm at higher temperatures for the bulkier system, *e.g.* after initial (HMDS)$_2$Ca···(H)C{CiPr(NDip)}$_2$Ca backbone coordination in an intermediate, as part of an anionic ligand exchange mechanism.[53]

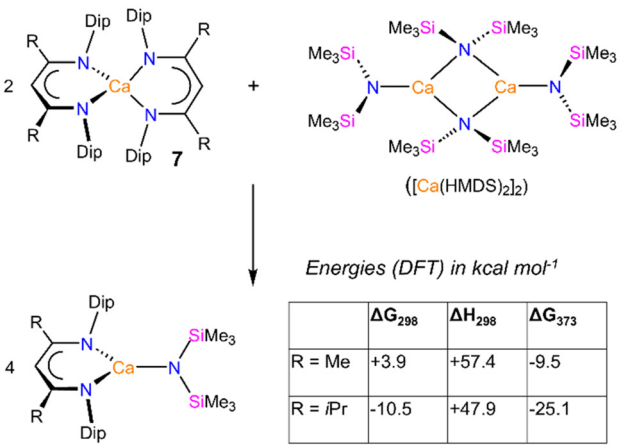

	ΔG_{298}	ΔH_{298}	ΔG_{373}
R = Me	+3.9	+57.4	-9.5
R = *i*Pr	-10.5	+47.9	-25.1

Fig. 7 DFT-calculated energies (B3LYP$_{PCM(benzene)}$/6-311G**//B3LYP/6-31G**) for the redistribution reaction to heteroleptic [(BDI)Ca(HMDS)] complexes. Note that the values are given for the formation of 4 moles of [(BDI)Ca(HMDS)].

3. Conclusions

In conclusion, the synthesis of a heteroleptic calcium amide [(^{iPrDip}BDI)Ca(HMDS)] **5** *via* the manipulation of the Schlenk-type equilibrium to destabilise a normally "kinetically inert" homoleptic species [(^{iPrDip}BDI)$_2$Ca] **7** has been presented. This ligand redistribution is made possible by the thermodynamic destabilisation of the homoleptic species [(^{iPrDip}BDI)$_2$Ca] relative to the heteroleptic congener, enabled by careful ligand modification. A one-pot system has been developed harnessing this ligand redistribution, which directly affords the heteroleptic calcium amide complex [(^{iPrDip}BDI)Ca(HMDS)] **5** from the reaction of the potassium complex [(^{iPrDip}BDI)K] **6**, calcium iodide and Ca(HMDS)$_2$ in a non-coordinating solvent in good yield. Insights into ligand redistribution strategies like in the presented case are also of interest for the stability and possible regeneration of catalytically competent heteroleptic complexes as part of catalytic cycles and to suppress complex decomposition pathways. Complex **5** has also been used as a precursor species to the new donor solvent-free calcium hydride complex [{(^{iPrDip}BDI)CaH}$_2$] **9**, which has been found to be substantially more thermally stable to Schlenk-type redistribution than [{(^{MeDip}BDI)CaH}$_2$]. Further investigation of the reactivity of compound **9** is ongoing, with the application of this thermally promoted Schlenk-type redistribution towards heavier alkaline earth metals also subject to investigation.

Author contributions

MdVT: investigation, formal analysis, computational analysis, writing – original draft. AMZS, DBC: X-ray crystallography, validation, data curation. AS: writing, visualisation, supervision, funding acquisition, conceptualisation.

Conflicts of interest

The authors have no conflicts to declare.

Data availability

Selected data that support the findings of this study are available in the supplementary information (SI). Supplementary information: research data (NMR spectroscopy, DFT computational studies) supporting this publication can be accessed at https://doi.org/10.17630/e377abd1-b331-464b-b555-1214950834ea. See DOI: https://doi.org/10.1039/d5dt02949j.

CCDC 2514137–2514141 contain the supplementary crystallographic data for this paper.[54a–e]

Acknowledgements

We would like to thank the Centre for Doctoral Training in Critical Resource Catalysis (CRITICAT, EP/L016419/1) for financial support and acknowledge use of the high-performance computing cluster CREATE (King's Computational Research, Engineering and Technology Environment). We acknowledge support for the St Andrews Single-Crystal X-Ray Diffraction Service from the University of St Andrews Strategic Equipment Fund.

References

1 S. Harder, *Chem. Rev.*, 2010, **110**, 3852–3876.
2 M. R. Crimmin and M. S. Hill, *Homogeneous catalysis with organometallic complexes of group 2*, 2013, vol. 45.
3 W. Schlenk and W. Schlenk, *Ber. Dtsch. Chem. Ges. A*, 1929, **62**, 920–924.
4 C. Lambert and P. von Ragué Schleyer, *Angew. Chem., Int. Ed. Engl.*, 1994, **33**, 1129–1140.
5 K. M. Birkhoff, I. Lin and S. Yruegas, *Inorg. Chem.*, 2025, **64**, 8185–8197.
6 A. Causero, G. Ballmann, J. Pahl, H. Zijlstra, C. Färber and S. Harder, *Organometallics*, 2016, **35**, 3350–3360.
7 Y. Tsai, *Coord. Chem. Rev.*, 2012, **256**, 722–758.
8 L. Bourget-Merle, M. F. Lappert and J. R. Severn, *Chem. Rev.*, 2002, **102**, 3031–3066.
9 D. C. H. Do, A. Keyser, A. V. Protchenko, B. Maitland, I. Pernik, H. Niu, E. L. Kolychev, A. Rit, D. Vidovic, A. Stasch, C. Jones and S. Aldridge, *Chem. – Eur. J.*, 2017, **23**, 5830–5841.
10 C. Jones, *Nat. Rev. Chem.*, 2017, **1**, 0059.
11 S. P. Sarish, S. Nembenna, S. Nagendran and H. W. Roesky, *Acc. Chem. Res.*, 2011, **44**, 157–170.
12 Y. Liu, J. Li, X. Ma, Z. Yang and H. W. Roesky, *Coord. Chem. Rev.*, 2018, **374**, 387–415.
13 D. B. Kennedy, M. J. Evans, D. D. L. Jones, J. M. Parr, M. S. Hill and C. Jones, *Chem. Commun.*, 2024, **60**, 10894–10897.
14 A. G. M. M. Barrett, M. R. Crimmin, M. S. Hill and P. A. Procopiou, *Proc. R. Soc. A*, 2010, **466**, 927–963.
15 M. Arrowsmith and M. S. Hill, *Alkaline Earth Chemistry: Applications in Catalysis*, Elsevier Ltd., 2013.
16 M. Arrowsmith, in *Encyclopedia of Inorganic and Bioinorganic Chemistry*, John Wiley & Sons, Ltd, Chichester, UK, 2015, pp. 1–26.
17 M. S. Hill, D. J. Liptrot, C. Weetman and M. S. Hill, *Chem. Soc. Rev.*, 2016, **45**, 972–988.
18 Y. Sarazin and J. F. Carpentier, *Chem. Rec.*, 2016, **16**, 2482–2505.
19 M. Magre, M. Szewczyk and M. Rueping, *Curr. Opin. Green Sustain. Chem.*, 2021, **32**, 100526.
20 M. Magre, M. Szewczyk and M. Rueping, *Chem. Rev.*, 2022, **122**, 8261–8312.
21 B. Rösch, T. X. Gentner, J. Langer, C. Färber, J. Eyselein, L. Zhao, C. Ding, G. Frenking and S. Harder, *Science*, 2021, **371**, 1125–1128.
22 J. Mai, M. Morasch, D. Jędrzkiewicz, J. Langer, B. Rösch and S. Harder, *Angew. Chem., Int. Ed.*, 2023, **62**, e202212463.
23 J. Mai, B. Rösch, J. Langer, S. Grams, M. Morasch and S. Harder, *Eur. J. Inorg. Chem.*, 2023, **26**, e202300421.
24 S. Thum, J. Mai, N. Patel, J. Langer and S. Harder, *ChemistryEurope*, 2025, **3**, e202500080.
25 M. Morasch, T. Vilpas, N. Patel, J. Maurer, S. Thum, M. A. Schmidt, J. Langer and S. Harder, *Angew. Chem., Int. Ed.*, 2025, **64**, e202506989.
26 A. S. S. S. Wilson, M. S. Hill, M. F. Mahon, C. Dinoi and L. Maron, *Science*, 2017, **358**, 1168–1171.
27 A. S. S. S. Wilson, C. Dinoi, M. S. Hill, M. F. Mahon and L. Maron, *Angew. Chem., Int. Ed.*, 2018, **57**, 15500–15504.
28 J. Dyall, M. S. Hill, M. F. Mahon, L. Teh and A. S. S. S. Wilson, *Dalton Trans.*, 2019, **48**, 4248–4254.
29 A. S. S. Wilson, C. Dinoi, M. S. Hill, M. F. Mahon, L. Maron and E. Richards, *Angew. Chem., Int. Ed.*, 2020, **59**, 1232–1237.
30 K. G. Pearce, C. Dinoi, M. S. Hill, M. F. Mahon, L. Maron, R. S. Schwamm and A. S. S. S. Wilson, *Angew. Chem., Int. Ed.*, 2022, **61**, e202200305.
31 K. Watanabe, J. H. Pang, R. Takita and S. Chiba, *Chem. Sci.*, 2022, **13**, 27–38.
32 K. G. Pearce, S. E. Neale, C. L. McMullin, M. F. Mahon and M. S. Hill, *Chem. Commun.*, 2024, **60**, 7882–7885.
33 J. J. C. Struijs, M. A. Ellwanger, A. E. Crumpton, V. Gouverneur and S. Aldridge, *Nat. Chem.*, 2024, **16**, 1473–1480.
34 M. J. Evans and C. Jones, *Chem. Soc. Rev.*, 2024, **53**, 5054–5082.
35 M. H. Chisholm, J. Gallucci and K. Phomphrai, *Chem. Commun.*, 2003, **384**, 48–49.
36 M. R. Crimmin, M. S. Hill, P. B. Hitchcock and M. F. Mahon, *New J. Chem.*, 2010, **34**, 1572.
37 T. X. Gentner, B. Rösch, K. Thum, J. Langer, G. Ballmann, J. Pahl, W. A. Donaubauer, F. Hampel and S. Harder, *Organometallics*, 2019, **38**, 2485–2493.

38 C. Bourne, H. Dong, K. McKain, L. C. Mayer, A. P. McKay, D. B. Cordes, A. M. Z. Z. Slawin and A. Stasch, *Dalton Trans.*, 2024, **53**, 9887–9895.
39 S. Burnett, C. Bourne, A. M. Z. Z. Slawin, T. van Mourik and A. Stasch, *Angew. Chem., Int. Ed.*, 2022, **61**, e202204472.
40 S. Thompson, S. Burnett, R. Ferns, T. van Mourik, A. P. McKay, A. M. Z. Slawin, D. B. Cordes and A. Stasch, *J. Am. Chem. Soc.*, 2025, **147**, 5247–5257.
41 S. J. Bonyhady, C. Jones, S. Nembenna, A. Stasch, A. J. Edwards and G. J. McIntyre, *Chem. – Eur. J.*, 2010, **16**, 938–955.
42 S. Harder, *Organometallics*, 2002, **21**, 3782–3787.
43 M. H. Chisholm, J. C. Gallucci and K. Phomphrai, *Inorg. Chem.*, 2004, **43**, 6717–6725.
44 R. D. Shannon, *Acta Crystallogr., Sect. A*, 1976, **32**, 751–767.
45 A. Poater, B. Cosenza, A. Correa, S. Giudice, F. Ragone, V. Scarano and L. Cavallo, *Eur. J. Inorg. Chem.*, 2009, 1759–1766.
46 L. Falivene, R. Credendino, A. Poater, A. Petta, L. Serra, R. Oliva, V. Scarano and L. Cavallo, *Organometallics*, 2016, **35**, 2286–2293.
47 *Handbook of Chemistry and Physics*, ed. W. M. Haynes, CRC Press, Florida, 61st edn, 1981.
48 S. Harder, *Chem. Commun.*, 2012, **48**, 11165.
49 M. M. D. Roy, A. A. Omaña, A. S. S. Wilson, M. S. Hill, S. Aldridge and E. Rivard, *Chem. Rev.*, 2021, **121**, 12784–12965.
50 S. Harder and J. Brettar, *Angew. Chem., Int. Ed.*, 2006, **45**, 3474–3478.
51 D. Mukherjee, D. Schuhknecht and J. Okuda, *Angew. Chem., Int. Ed.*, 2018, **57**, 9590–9602.
52 A. Causero, G. Ballmann, J. Pahl, C. Färber, J. Intemann and S. Harder, *Dalton Trans.*, 2017, **46**, 1822–1831.
53 S. R. Lawrence, D. B. Cordes, A. M. Z. Slawin and A. Stasch, *Dalton Trans.*, 2019, **48**, 16936–16942.
54 (*a*) CCDC 2514137: Experimental Crystal Structure Determination, 2025, DOI: 10.5517/ccdc.csd.cc2qd56j; (*b*) CCDC 2514138: Experimental Crystal Structure Determination, 2025, DOI: 10.5517/ccdc.csd.cc2qd57k; (*c*) CCDC 2514139: Experimental Crystal Structure Determination, 2025, DOI: 10.5517/ccdc.csd.cc2qd58l; (*d*) CCDC 2514140: Experimental Crystal Structure Determination, 2025, DOI: 10.5517/ccdc.csd.cc2qd59m; (*e*) CCDC 2514141: Experimental Crystal Structure Determination, 2025, DOI: 10.5517/ccdc.csd.cc2qd5bn.